Canadian Mineralogist
Vol. 25, pp. 37-50 (1987)

MASSIVE-SULFIDE FABRICS AT KAMBALDA AND THEIR RELEVANCE TO THE INFERRED STABILITY OF MONOSULFIDE SOLID-SOLUTION

ALISTAIR COWDEN† AND NICHOLAS J. ARCHIBALD*

Geological Research Laboratory, Western Mining Corporation Limited, Kambalda Nickel Operations, Kambalda, Western Australia 6442, Australia

Abstract

The Kambalda area has undergone lower amphibolite facies metamorphism and complex polyphase deformation. Fe–Ni sulfides represent variably altered and deformed relict magmatic sulfides. Fabric relationships in massive sulfides mimic tectonite fabrics in adjacent silicate assemblages and indicate that sulfide fabrics preserve the total deformational sequence. Pyrrhotite–pentlandite layering in massive sulfides of low and medium Ni-tenor developed as an S_1 fabric in response to ductile, noncataclastic deformation. This deformation also produced flattened foliated lenses of relict magmatic pyrite. During D_2 deformation, a second-generation fabric (S_2) developed in high-strain domains, resulting in extreme cases in the formation of a totally transposed layering. An upright S_3 spaced cleavage, coincident with metamorphic peak, overprints these fabrics. Marginal pyrite selvedges represent replacement of pyrrhotite through sulfurization at the edges of the massive sulfide layer. Coarse-grained idioblastic pyrite overprints pyrrhotite–pentlandite layering, marginal pyrite selvedges and relict magmatic pyrite lenses. Pyrite replacement of pyrrhotite and recrystallization are synchronous with retrograde metamorphism. The fabric evidence suggests that prograde metamorphic events did not result in a complete reversion to monosulfide solid-solution, contrary to the conclusions of previous workers. A new interpretation of experimental data supports this inference, and indicates that the stable assemblage, for typical medium-tenor ores at lower amphibolite facies, is: nickeliferous pyrrhotite + nickel-rich monosulfide solid-solution.

Keywords: sulfide fabrics, nickel sulfides, metamorphism, deformation, Kambalda, Australia.

Sommaire

La région de Kambalda a été soumise à un métamorphisme de facies amphibolite inférieur et à une déformation polyphasée complexe. Les sulfures Fe–Ni sont des reliques magmatiques altérées et déformées à des degrés divers. Les relations texturales entre sulfures massifs simulent la texture des tectonites que l'on observe dans les assemblages de silicates avoisinants et indiquent que la texture des sulfures a préservé, dans son entièreté, la suite des déformations. Les couches superposées de pyrrhotine–pentlandite, dans les sulfures massifs à basse ou moyenne teneur en nickel, se sont formées en texture S_1 sous l'action d'une déformation ductile et non-cataclastique. Cette même déformation a également produit des masses lenticulaires, feuilletées et aplaties, de pyrite magmatique résiduelle. Au cours de la déformation D_2, une texture de deuxième génération (S_2) s'est formée dans les domaines fortement déformés, provoquant, dans les cas extrêmes, la transposition totale des couches. Un système de joints verticaux, espacés de S_3, marquant le maximum du métamorphisme, traversent les textures précitées. Des liserés de pyrite marginale témoignent du remplacement de la pyrrhotine par sulfurisation en bordure de la couche de sulfure massif. De la pyrite idioblaste à grain grossier vient se superposer à l'ensemble couches de pyrrhotine–pentlandite, liserés de pyrite marginale et lentilles de pyrite magmatique résiduelle. Le remplacement de la pyrrhotine par de la pyrite avec recristallisation est contemporain du métamorphisme rétrograde. Les faits texturaux observés montrent que le métamorphisme prograde n'a pas eu pour résultat le retour total à une solution solide de monosulfure, ce qui est contraire aux conclusions des auteurs antérieurs. La nouvelle interprétation des données expérimentales étaye la conclusion que l'assemblage stable des minerais typiques, à teneur moyenne et de facies amphibolite inférieur, est: pyrrhotine nickelifère + solution solide de monosulfure riche en nickel.

(Traduit par la Rédaction)

Mots-clés: texture des sulfures, sulfures de nickel, métamorphisme, déformation, Kambalda, Australie.

Introduction

The Kambalda Fe–Ni sulfide deposits occur in the Norseman–Wiluna belt, a NNW-trending Archean greenstone belt within the Yilgarn Block of Western Australia. The deposits are well documented (*e.g.*, Ewers & Hudson 1972, Ross & Hopkins 1975, Gresham & Loftus-Hills 1981, Marston 1984), and are regarded as the type example of the komatiite-associated nickel deposits (Marston *et al.* 1981).

The association of the deposits with komatiite lavas has influenced most investigators to conclude that the deposits are magmatic in origin, and formed by the accumulation of settling immiscible Fe–Ni sulfide droplets within komatiite flow-units. Recent publications have concentrated on the origin and geometry of these komatiite host-rocks (*e.g.*, Lesher

†Present address: Department of Geology, Private Bag, University of Auckland, Auckland, New Zealand.

*Present address: c/o Exploration House, 229 Stirling Highway, Perth, Claremont, Western Australia 6010, Australia.

et al. 1981, 1984), or the mechanisms of magma flow and cooling (*e.g.*, Huppert *et al.* 1984). Significantly, however, Barrett *et al.* (1976, 1977) and Groves *et al.* (1979) highlighted the potential importance of metamorphic modification, and pointed out that the extent of any metamorphic overprint must be clearly understood before an attempt is made to model magmatic processes.

This paper concentrates on i) the role of deformation and metamorphism in producing the characteristic textures of the massive-sulfide ores and, ii) the way in which these processes can explain the nature and origin of pyrrhotite–pentlandite layering and of pyrite selvedges and lenses within massive sulfides. An alternative interpretation of experimental phase-relationships in the Fe–Ni–S system is presented to allow for the development and preservation of tectonite layering in massive-sulfide ores during prograde amphibolite-facies metamorphism.

Geology of the Deposits

The volcanic stratigraphy and nature of the Kambalda deposits are described by Ross & Hopkins (1975), Gresham & Loftus-Hills (1981), Groves & Hudson (1981) and Marston (1984). In this section, only those aspects relevant to this paper are summarized.

Metamorphic and tectonic framework

The Kambalda area has a complex tectonic-metamorphic history, with polyphase deformation accompanying prograde metamorphism. The main phases of deformation are associated with the development of structures and tectonite fabrics at all scales; this produced complex geometries of form surfaces. All rocks at Kambalda have been metamorphosed; however, for clarity all meta- prefixes will be omitted.

The only published accounts of the metamorphic and tectonic histories for the Kambalda region are those of Barrett *et al.* (1977) and Gresham & Loftus-Hills (1981). Systematic remapping of underground, surface and diamond-drill information, combined with petrological data from up to 500 thin sections, has provided a complete re-interpretation of the stratigraphic, metamorphic and tectonic framework of the Kambalda area. These data are reported in an unpublished Western Mining Corporation report (Archibald 1985) and will be described in a subsequent paper. In this paper only a summary of this framework is given.

D_1: The earliest recognized deformational phase at Kambalda is interpreted to be a major thrusting event. Folds are rarely observed, and S_1 fabrics are weakly to strongly developed as foliations parallel or subparallel to lithological layering. Strain associated with D_1 is dominantly constrictional away from shear zones. Examples of D_1 thrusts are the Juan Fault (Marston & Kay 1980) and the Foster thrust (Fig. 4, Gresham & Loftus-Hills 1981).

D_2: This event produced open to tight, recumbent to inclined folds, commonly dislocated by extensive thrusts parallel or subparallel to their axial surfaces. A prograde tectonite fabric was heterogeneously developed during D_2. Strain was dominantly flattening. Most pinchouts (Gresham & Loftus-Hills 1981) are examples of this deformation, for example along the western margin of Hunt shoot (see Fig. 3B, Gresham & Loftus-Hills 1981).

D_3: This deformation produced open, upright folds such as the Kambalda dome (Gresham & Loftus-Hills 1981). Associated axial-surface foliations are irregularly developed as NNW-trending spaced cleavage. Deformation was synchronous with to slightly later than the peak of metamorphism. This deformation is equivalent to the D_3 of Archibald *et al.* (1978).

D_4: Deformation associated with this event is restricted to major upright NNW-trending normal and reverse faults. Related tectonite fabrics are retrograde. Examples are the Boulder–Lefroy fault (Gresham & Loftus-Hills 1981) and the Hunt A fault (Phillips & Groves 1984).

Metamorphic conditions at Kambalda attained the lower amphibolite facies. A combined estimate of peak metamorphic conditions of 520–550°C and 2.5 ± 1 kbar is based on the work of Bavinton (1979, 1981), Donaldson (1983) and Archibald (1985).

Nickel sulfide mineralization

The stratigraphy of mafic and ultramafic rocks intimately associated with nickel mineralization is relatively simple, comprising a thick sequence of tholeiitic basalts, which is overlain by a series of komatiite flow-units. The komatiites can be divided into an upper member, consisting of thin (1–2 m) flow units of moderate Mg-content (16–30% MgO), and a lower member, consisting of thick (50 m), high-Mg flow units (30–40% MgO) and interflow sediments. The nickel mineralization occurs toward the base of the lower member as thin, tabular concentrations of Fe–Ni sulfides of varying tenor. Tenor is defined as nickel in 100% sulfides; low-tenor ores contain less than 8% Ni, medium-tenor ores between 8 and 14% Ni, and high-tenor ores, greater than 14% Ni (see Cowden & Woolrich 1987). Ore 'shoots' consist of one or more of these tabular sulfide bodies, many of which are structurally dislocated into a number of ore surfaces. Broadly, three distinct categories can be delimited, based on their stratigraphic and structural settings. These are contact, hanging-wall and offset ores (Gresham & Loftus-Hills 1981).

Contact ores occur at the base of the first ultramafic flow-unit immediately overlying the basalt footwall. Typically this ore type is in part confined to embayments, or troughs, in the footwall basalt. The margins of the embayments are termed pinch-outs and in most cases are D_2 low-angle reverse thrusts or tight recumbent folds. The bulk of the nickel reserves at Kambalda (Gresham & Loftus-Hills 1981) occur as large-tonnage, medium-tenor, contact ore-shoots such as Long, Lunnon and Juan shoots (Gresham 1986). Hanging-wall ores occur at the base of the second komatiite flow-unit or, less commonly, at the base of the third or fourth flow-unit. They typically overlie contact-ore positions, contain less nickel metal and are higher in tenor than their respective underlying contact-ores. Offset ores form a minor component of the metal reserves, albeit locally important. As the term implies, they have been structurally emplaced into an offset position in the footwall or hanging-wall of a major orebody.

The ore zone

The ore zone is one to five metres thick and comprises varying proportions of massive, matrix and disseminated sulfides (Fig. 1). Massive sulfides contain greater than 80% sulfides, matrix sulfides contain 40 to 80% sulfides, and disseminated sulfides contain 10 to 40% sulfides. Woodall & Travis (1969) first described the characteristic stratification of the ore zone, where matrix and disseminated sulfides overlie massive sulfides. Individual types of ore can occur in isolation, but generally there is evidence of tectonic disruption where this is the case.

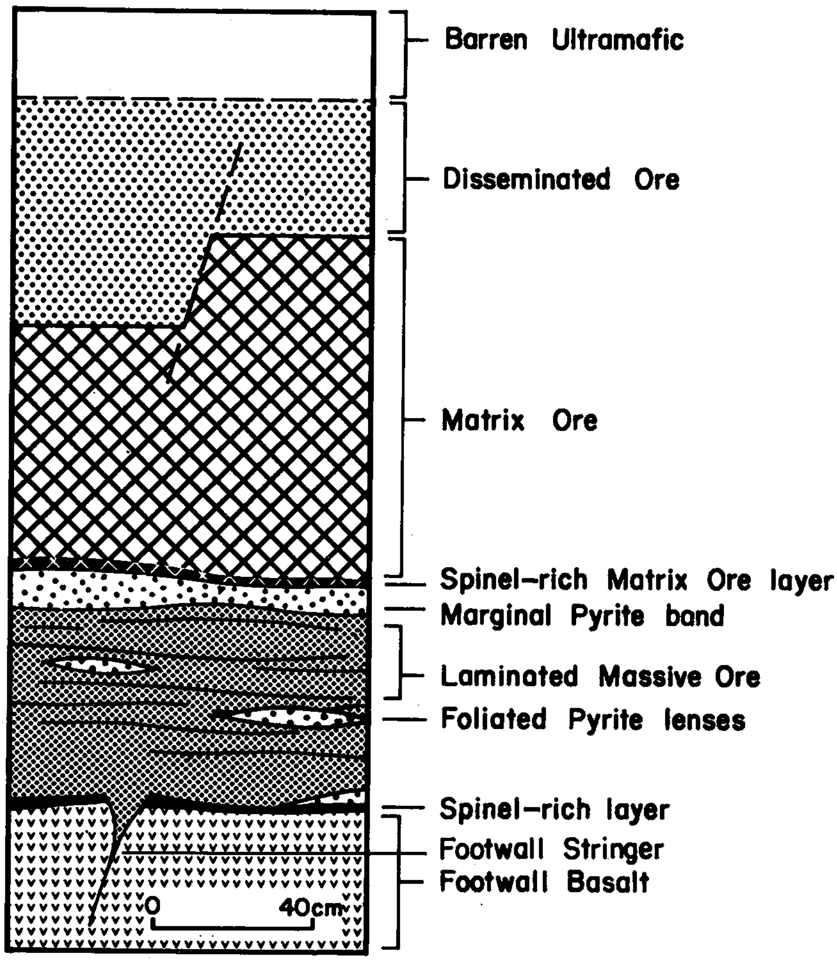

FIG. 1. A schematic sketch of a typical section through the ore zone.

Massive sulfides are most common as low- and medium-tenor contact ores and usually comprise 30% of the ore profile. Typically, they form a near-continuous irregular layer on the footwall basalt; their local distribution is controlled by small-scale structural features such as faults or folds (Marston & Kay 1980). In both contact and hanging-wall high-tenor ore surfaces, massive sulfides are less common and have a more irregular distribution than associated disseminated ores.

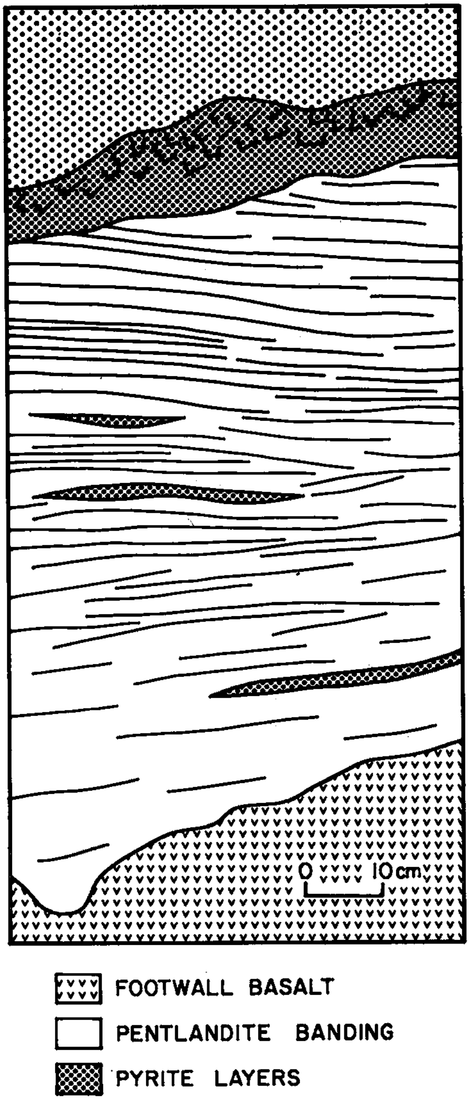

FIG. 2. Sketch of well-layered, medium-tenor massive sulfides from 1204 south stope, Juan Main surface, Juan complex, (KNO grid co-ordinates 551340N, 371510E, – 50 m R.L.). Note the upper marginal pyrite selvedge transgressing layering and the internal pyrite lenses.

Pyrrhotite–pentlandite layering is characteristic of massive sulfides, particularly in low- and medium-tenor ores. It grossly parallels the overall attitude of the massive-ore layer. Pyrite is common and occurs as discrete layers or lenses, either within or at the margins of the massive-sulfide layer (Fig. 1). Magnetite and chromite are minor accessory minerals, and are concentrated at the top or bottom of the massive-sulfide layer (Fig. 1).

Matrix and disseminated sulfides generally form a more continuous and thicker layer overlying massive sulfides. The contact between the two is sharp, and commonly tectonic. The mineralogy of matrix and disseminated sulfides is similar to that of massive sulfides, consisting of pyrrhotite, pentlandite, pyrite and magnetite. However, magnetite and, to a lesser extent, chromite, are more abundant in these rocks compared to massive sulfides (Ewers & Hudson 1972). Matrix and disseminated sulfides do not exhibit the marked textures and fabrics of massive sulfides.

FABRIC ELEMENTS AND TEXTURES IN MASSIVE SULFIDES

Two important features of massive sulfides, namely pyrrhotite–pentlandite layering and pyrite layers and lenses, have important implications for interpretation of the deformation history of massive sulfides.

Pyrrhotite–pentlandite layering

In the following sections, the fabrics of massive sulfides are described, covering the range from early-formed ductile tectonite fabrics and their development, to the effects that late-stage brittle fractures have in modifying the ore profile.

Previous investigators (*e.g.*, McQueen 1979a,b, Groves & Hudson 1981) have suggested that the layering is a late-metamorphic fabric following unmixing from a single-phase monosulfide solid-solution (*Mss*) (*cf.* Naldrett *et al.* 1967, Kullerud *et al.* 1969) synchronous with or after the peak of metamorphism. Gross fabric relationships observed from many underground faces, however, indicate a more complex origin.

Layering dominates most low- and medium-tenor massive sulfides, and consists of alternating layers of pyrrhotite and pentlandite that are commonly parallel to the margins of the massive-sulfide layer (Fig. 2; Woodall & Travis 1969, Ewers & Hudson 1972, Ross & Hopkins 1975, Marston & Kay 1980). This fabric represents an annealed tectonite (Bayer & Siemes 1971, Barrett *et al.* 1977, Ostwald & Lusk

1978). Mineralogical layering is poorly developed in high-tenor ores, but strong contact-parallel *fabrics* are common. As these rocks underwent the same deformations as medium-tenor ores, the lack of development of layering is attributed to their high content of pentlandite and pyrite (Cowden & Woolrich 1987).

The development of layering from crackle-veined massive sulfides is described. This latter type of ore is rare and consists of pyrrhotite criss-crossed by a network of fractures, infilled by fine-grained pentlandite (Figs. 3, 4B), and discrete amoeboid aggregates of fine-grained pyrite (average 5 cm in diameter). The pyrrhotite apparently occurs as large (10 cm) single crystals. In all cases where crackle-veined massive sulfides have been observed (*e.g.*, 50 and 52 surfaces at the Juan complex, and on the 7, 8 and 9 levels at Long shoot), they are within the central portion of the massive-sulfide layer and never at the margins. In the 1050 stope at the Juan complex, crackle-veined sulfides grade into layered massive-sulfides on the footwall contact, and the discrete amoeboid aggregates of pyrite are progressively flattened and foliated toward the base. The development of mineralogical layering and flattening of pyrite with progressively increasing strain is illustrated in Figure 3. This sketch shows a rock transitional in texture between crackle-veined and layered sulfide. The timing of the development of this layering is constrained by the overprint of an upright, S_3 spaced cleavage (Fig. 3), and is therefore related to either the D_1 or D_2 deformation.

Tight folds of massive-sulfide layering are common and typically occur in the hinge zones of F_2 folds (*e.g.*, pinchouts). These folds rarely have any expression in the upper and lower margins of the massive ores. An example from Fisher shoot (Fig. 4D) illustrates the development of an S_2 axial-surface foliation in the hinge zone of a mesoscopic F_2 fold in layered sulfides. Fine-grained foliated lenses of pyrite, flattened in S_1, are folded, and S_2 is developed as a second-generation layering. This mesoscopic fold is parasitic to a macroscopic overturned F_2 syncline (the Fisher Trough, Gresham & Loftus-Hills 1981). Another example is illustrated in Figure 5, where at Hunt shoot, inclined F_2 folds of the basalt–komatiite contact define the 'pinchouts' to the ore surfaces. In the hinge zone of the folds, pillows in the footwall basalt are flattened in the plane of a strong S_2 foliation with pillow elongation paralleling the pitchline of this pinchout. The strong S_2 foliation obliterates S_1 banding in massive sulfides, with pyrite lenses reoriented and flattened in S_2. In other localities, for example at Long shoot, fine-grained elongate lenses of pyrite occur at an angle to the dominant mineralogical layering (see also Seccombe *et al.* 1981). This is interpreted to represent extreme transposition, such that the only preserva-

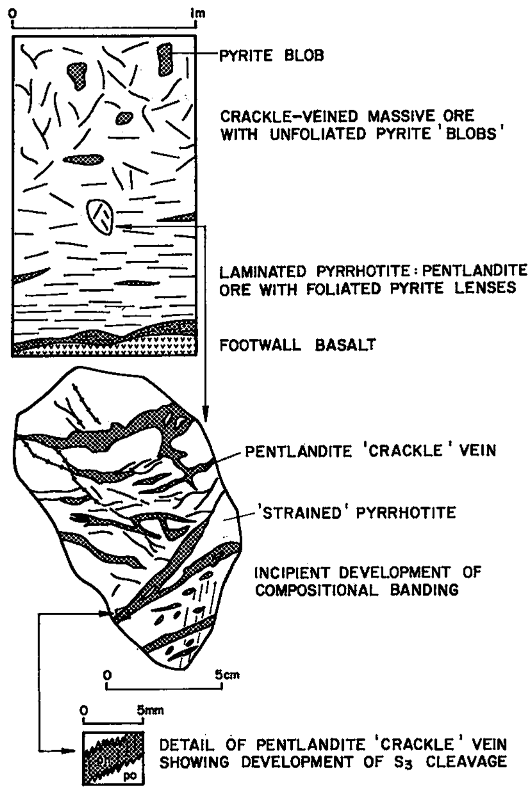

FIG. 3. Sketch of medium-tenor sulfides from the 1050 stope, 50 surface, Juan complex (KNO grid co-ordinates 55139&N, 371703E, +88 m R.L.), showing the progressive development of banded massive sulfides from crackle-veined massive sulfides. Note the flattening of amoeboid pyrite blobs and the overprinted S_3 cleavage.

tion of the S_1 fabric occurs in the pyrite lenses, with the massive ore exhibiting a strong S_2 banding. Both these examples illustrate that fabrics in sulfides are congruent with those in adjacent silicate rocks.

Brittle fracture of the basalts in the immediate footwall affects overlying massive-sulfides. Sulfides are injected into these fractures, flowing plastically around basalt contacts and deforming pyrrhotite-pentlandite banding. These structures typically developed during either D_2 or D_3; in the latter case the small faults and offsets are generally parallel to S_3.

Fabric relationships in the massive sulfides mimic tectonite fabrics in adjacent silicate assemblages and indicate that the sulfide fabrics preserve the total deformational sequence. Most of the pyrrhotite-pentlandite layering developed as an S_1 fabric. During the D_2 deformation, an S_2 fabric was developed in higher-strain domains such as flattened F_2 hinge zones and resulted, in extreme cases, in the formation of a totally transposed layering. Thus there is

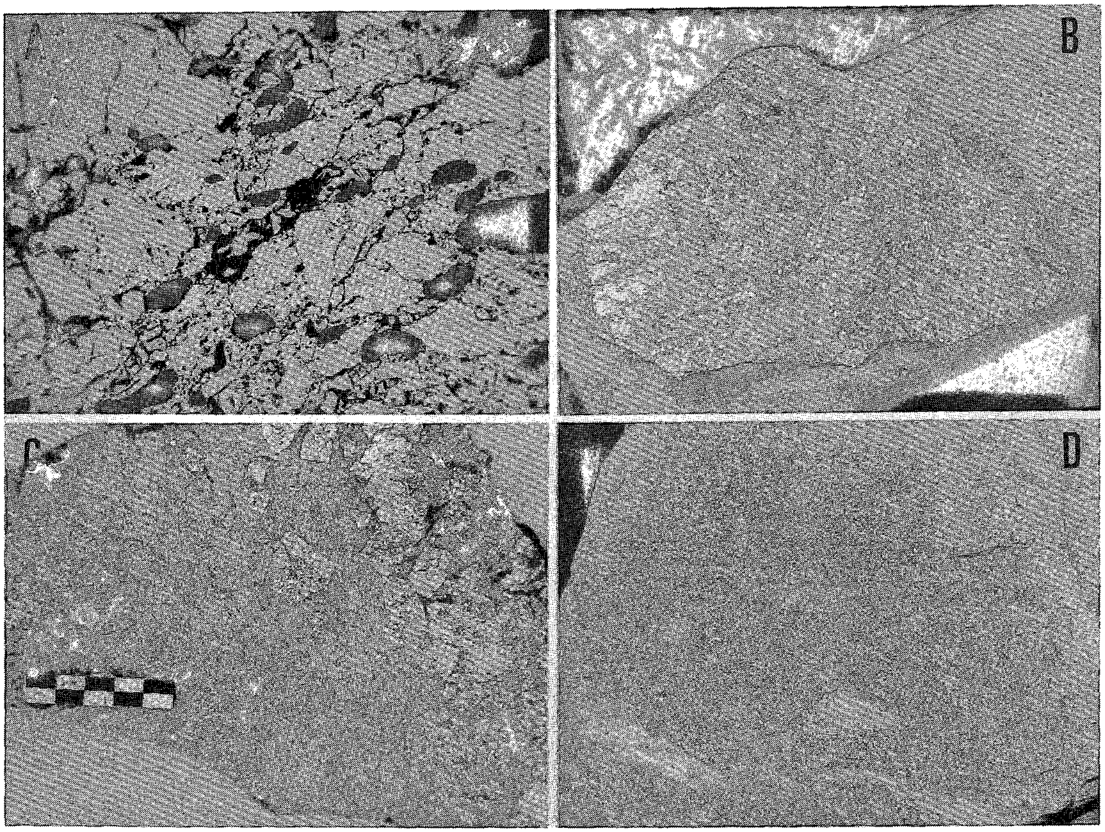

FIG. 4. Photographs of textures in medium-tenor massive sulfides. A. Photomicrograph of boundary of marginal pyrite selvedge with a pyrrhotite layer in massive sulfides. Sample is from face sketched in Figure 2. Pyrite to the right invades grain boundaries between pyrrhotite (left), eventually isolating and consuming pyrrhotite. Sample Z18808. B. Crackle-veined massive sulfides from the 1050 stope; massive sulfides sketched in Figure 3. Fractures or veins in pyrrhotite are filled by fine-grained pentlandite. Sample Z24323. C. Part of a large lens of fine-grained foliated pyrite (type 3) in massive sulfides from the 1104 stope, Juan Main surface, Juan complex. Foliation in the fine-grained pyrite is defined by elongate inclusions of silicates and carbonates. Coarse idioblastic pyrite (type 6) overgrows this foliation. Note that the idioblastic pyrite occurs in close association with chalcopyrite in the central portion of the pyrite lens. Sample Z14747. D. Layered massive-sulfide from Fisher shoot, 14L decline, (KNO co-ordinates 546927N, 372311E, −154 R.L.). Specimen shows F_2 fold of S_1 layering and transposition of layering to form an S_2 banding axial planar to the F_2 fold. Note the re-orientation of flattened lenses of foliated pyrite. Sample Z27515.

extensive field-evidence that tectonite layering in the sulfides developed predominantly as D_1 and D_2 fabrics and, consequently, prior to the peak of metamorphism (Archibald 1985). Further evidence is provided by the layer-parallel nature of pyrrhotite–pentlandite layering where the geometry of this layering is highly variable, yet the S_3 (peak of metamorphism) fabric is constantly an upright NNW cleavage.

Development of layering

The observations on the development of layering in massive sulfides have very important genetic implications. Most experimental work (Naldrett *et al.* 1967, Kullerud *et al.* 1969) suggests that at peak metamorphic conditions at Kambalda the only stable phase for most ore compositions is *Mss*. Previous interpretations of the mineralogical layering in massive sulfides (Barrett *et al.* 1977, McQueen 1979a,b, Groves & Hudson 1981) claim that layering resulted from nucleation and exsolution of pentlandite from this *Mss* during cooling from the peak metamorphic conditions.

The textural evidence presented in this paper suggests that pyrrhotite–pentlandite layering in massive sulfides was developed during D_1 and D_2 and was preserved through peak conditions (D_3). Subsequent exsolution, recrystallization and annealing during peak (D_3) and retrograde (D_4) metamorphism modified sulfide textures, but did not destroy the prograde (D_1–D_2) fabrics. The inference is that layering formed as a response to deformation and not from stress-directed exsolution upon cooling. Therefore, any model for the formation of layering is basically constrained by the same processes that control the development of banding in silicate rocks, such as mylonites or banded gneisses. Vernon (1974) concluded that to produce essentially monomineralic layers by ductile deformation, the precursor rock must have two basic properties: firstly, it must contain more than one mineral, and secondly, the grain size of the original rock must have been greater than that of the resultant tectonite. The development of layering in massive sulfides, outlined below, satisfies the constraints imposed by Vernon's model.

Layering in low- and medium-tenor massive sulfides formed from the deformation of a massive, coarse-grained, pyrrhotite – pentlandite ± pyrite assemblage, perhaps similar to crackle-veined massive sulfide. The development of different types of tectonite fabric as a response to varying degrees of stress is shown schematically in Figure 6. Deformation resulted in plastic flow and recrystallization of individual grains into elongate layers that were subsequently annealed. Constituent minerals responded differently to deformation: pyrrhotite deformed plastically, pentlandite, which is less ductile, retained its integrity as extensive layers, whereas pyrite, which is the least ductile, was drawn out into small lenses or bands.

Strain within a massive-ore profile was heterogeneous, being most intense adjacent to the footwall contact. This resulted in sulfide blastomylonites on the contact, and granoblastic sulfide gneisses away from this contact. The development of layering in massive sulfides is also dependent on the pentlandite-pyrrhotite ratio. Low- and medium-tenor ores are well layered, whereas high-tenor ores, which contain only minor pyrrhotite, are poorly layered. In part, this reflects the differing deformational properties of the constituent minerals; under ductile conditions, low- and medium-tenor pentlandite–pyrrhotite ores would have a lower strength at a given stress than high-tenor pentlandite–pyrite ores (*cf.* Barrett *et al.* 1977; MacDonald & Paterson, pers. comm., 1985). However, other important contributing factors are the phase relationships of high-tenor ore compositions at elevated temperatures (300–600°C).

Overall, the massive sulfides would behave as very low-strength materials under the P–T conditions estimated during deformation. They would have a high ductility and low strength compared to most silicate assemblages (Clark & Kelly 1973; J. MacDonald & M. Paterson, pers. comm., 1985), deforming plastically at much lower stresses than adjacent host-rocks. In this regard, it would be possible to produce, at comparatively low stresses, textures in massive ores

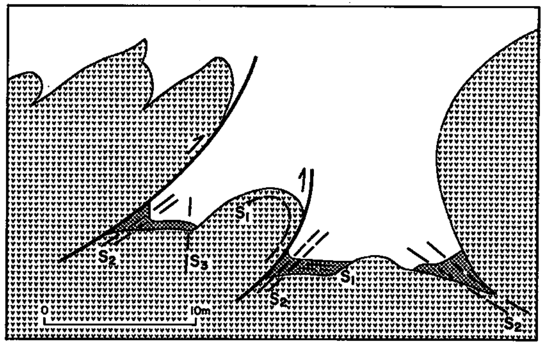

FIG. 5. Sketch cross-section of the D Zone Deeps area, Hunt shoot (cross section no. 84). Note the folding of an S_1 foliation by F_2 recumbent folds and obliteration of S_1 banding in sulfides by S_2 foliation associated with thrusting in pinchouts. Upright S_3 cleavage overprints these fabrics.

similar to those normally associated with extreme strain in silicate rocks, *i.e.*, ductile shear-zones in high-grade gneisses (Katz 1968, Ramsay & Graham 1970, Vernon 1974, Myers 1978).

Pyrite textures

Previous studies of nickel ores at Kambalda have identified two habits or modes of occurrence of pyrite in massive sulfides: coarse-grained pyrite is associated with chalcopyrite, and fine-grained pyrite is associated with pentlandite (Ewers & Hudson 1972, Marston & Kay 1980, Seccombe *et al.* 1981). This study has shown that the distribution and mode of occurrence of pyrite in massive sulfides are more complex than this; a summary of the various types

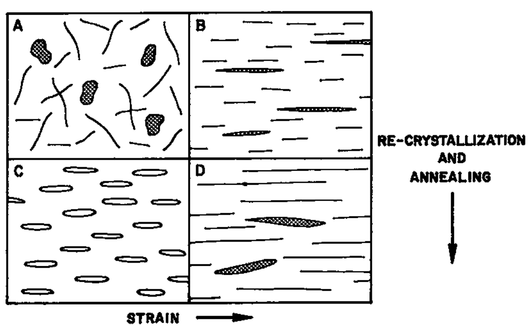

FIG. 6. Textures in massive sulfides as a function of degree of stress and annealing. A. Coarse-grained, crackle-veined massive sulfide containing blobs of fine-grained pyrite. B. Fine-grained, foliated massive sulfides containing flattened foliated fine-grained pyrite lenses. C. Coarse-grained, poorly-banded massive sulfide. D. Coarse-grained, well-banded massive sulfide containing flattened foliated pyrite lenses.

of pyrite, together with their different textural and structural settings, follows:

Type 1: fine-grained pyrite forming an integral part of high-tenor ores. Pyrite is a primary component of high-tenor ores because their bulk composition lies within the field of coexisting pyrrhotite–pentlandite–pyrite in the Fe–Ni–S system (Cowden & Woolrich 1987). This contrasts with compositions of low- and medium-tenor ores, which lie on or near the pyrrhotite–pentlandite tie line (Cowden & Woolrich 1987). As a consequence, pyrrhotite-poor pentlandite–pyrite assemblages are common in high-tenor ores; pyrite is interstitial to pentlandite.

Type 2: amoeboid aggregates in medium-tenor crackle-veined sulfides. This type forms discrete amoeboid aggregates of fine-grained pyrite in crackle-veined massive sulfides.

Type 3: elongate lenses of foliated pyrite within massive sulfides. Fine-grained lenses of foliated pyrite are common in medium-tenor, layered massive-sulfides, in recrystallized, structureless massive-sulfides and especially so in high-tenor ores (Fig. 7). The lenses within medium-tenor massive sulfides are deformed equivalents of the amoeboid blobs in crackle-veined sulfides. They typically occur within the massive-sulfide layer, though layers of foliated pyrite along the margins have also been observed. Internal lenses are generally small, on average 5 × 2 cm, although rarely they attain several metres in length. They have a strong foliation defined by sutured, locally anastomosing aggregates of elongate pyrite, trains of pentlandite, magnetite and deformed silicate inclusions. The margins of these lenses are sharp, and there is no pyrite replacement of adjacent pyrrhotite in massive sulfides, together suggesting a deformed contact. An upright S_3 cleavage overprints pyrite lenses, although cleavage is not always well developed.

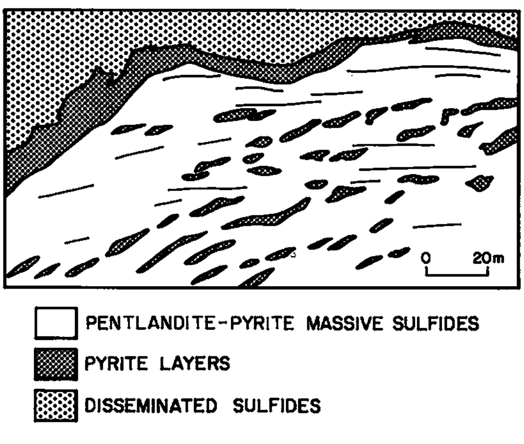

FIG. 7. Sketch of high-tenor massive sulfides from the 234 stope, Banana surface, Juan complex (KNO grid coordinates 550300N, 371595E, +281 R.L.). Foliated but poorly banded massive sulfides contain abundant fine-grained foliated pyrite lenses (type 3) resembling a flaser texture. Note the marginal pyrite band (type 4) at the upper massive-sulfide boundary.

Type 4: pyrite selvedges at the margins of massive-sulfide layers comprising both coarse- and fine-grained pyrite. Pyrite selvedges occur as thick (1 to 10 cm), impersistent layers at the margins of massive sulfides (Fig. 7). They are most commonly developed where massive sulfides are in contact with either matrix or disseminated sulfides (Fig. 2; see also Woodall & Travis 1969, Ewers & Hudson 1972). The pyrite selvedges mimic the margin of the massive sulfides, even where this margin is unequivocally tectonic, such as a D_3 fault offset (Fig. 2). The lower boundary of these selvedges is typically discordant to the pyrrhotite–pentlandite layering and appears sharp in hand specimen. On a microscopic scale, the boundary is gradational, with pyrrhotite in massive sulfides replaced by ragged, anhedral fine-grained pyrite (Fig. 4A). The pyrrhotite–pentlandite foliation is partially preserved as a 'ghost' foliation in marginal layers of pyrite. The relict layering within the pyrite selvedge is defined by sutured, elongate aggregates of pyrite after pyrrhotite, trains of magnetite and foliated gangue inclusions. Importantly, ovoid grains of magnetite aligned parallel to the layering in the massive sulfides show no change in abundance, orientation or morphology across the pyrite-banded sulfide boundary. Clearly, marginal selvedges of pyrite are superimposed upon pyrrhotite–pentlandite layering and appear to result from the alteration of pyrrhotite to pyrite *without* any coincident production of magnetite (Fig. 4A).

Internally the pyrite selvedges are not homogeneous and are commonly modified by subsequent recrystallization. Coarse, idioblastic pyrite grains (type 6), typically associated with chalcopyrite, are commonly well developed at the top of the selvedge (Fig. 4C). In contrast, fine-grained pyrite with associated pentlandite is predominant at the base of the band.

An upright S_3 cleavage is observed in layered sulfides, but is not generally developed in the marginal selvedges of pyrite. Either pyrite does not record this cleavage event, or formation of marginal pyrite selvedges is syn- to post-D_3.

Type 5: fine-grained pyrite around late brittle fractures. Fine-grained pyrite is developed in 1- to 2-cm wide selvedges around late (D_4?) brittle fractures that cross-cut massive sulfides. This style of replacement pyrite is similar to that of fine-grained pyrite in marginal selvedges.

Type 6: scattered coarse-grained idioblastic pyrite. Scattered idioblastic pyrite grains are developed throughout low- and medium-tenor massive sulfides, overprinting all pre-existing fabrics and resulting from late recrystallization of fine-grained pyrite or nucleation of new grains. Coarse-grained pyrite forms the core to larger fine-grained foliated pyrite lenses (type 3) and is common within the upper marginal selvedges of pyrite (type 4). It also overgrows pyrrhotite–pentlandite layered sulfides. Coarse-grained pyrite is rarely in contact with layered sulfide (Fig. 2) and in such cases, for example, at Long shoot, massive sulfides are completely altered and recrystallized to coarse (up to 10 cm) idioblastic pyrite grains in a matrix of pentlandite; commonly such ores are associated with thick marginal layers of magnetite.

These six types of pyrite can be considered in three categories within the context of a tectonic framework. Firstly, there is possible relict magmatic pyrite, either occurring as pyrite in high-tenor ore (type 1), as undeformed amoeboid aggregates (type 2) or as lenses deformed by the earliest D_1 and D_2 deformations (type 3). Secondly, there is metamorphic replacement pyrite occurring along the margins of massive ores or late brittle fractures (type 4 and 5). Thirdly, idioblastic grains of recrystallized pyrite are developed from all of the above categories or represent newly nucleated grains of idioblastic pyrite (type 6).

The first category (types 1, 2 and 3) is considered to have formed as an exsolved phase during cooling and crystallization of magmatic sulfides (Barrett *et al.* 1977). It is not considered here in more detail. The second and third categories modify a mineralogical banding formed as a tectonite fabric, and as such form late in the deformational-metamorphic history (syn- or post-D_3). Their development is discussed in more detail below.

Marginal selvedges of pyrite are interpreted as pyrite replacement of pyrrhotite without coincident generation of magnetite (see Fig. 4A). This suggests that a sulfurization reaction occurred similar to that outlined by Seccombe *et al.* (1981). Oxidation, as proposed by Marston & Kay (1980), would require the generation of substantial amounts of magnetite. Only in cases of extreme metamorphic modification of massive sulfides, for example in parts of Long shoot and Gibb shoot (see Cowden 1986), is there abundant magnetite associated with massive sulfides. In most cases massive sulfides contain about 2% magnetite (Ewers & Hudson 1972), and thus sulfurization appears to be the dominant process of alteration.

Seccombe *et al.* (1981) suggested that the sulfurization occurred as a result of the interaction of late metamorphic fluids with massive sulfides. The fabric evidence presented here confirms that such reactions occurred late in the tectonic history of the massive sulfides and wherever fluid access was possible (for example, along brittle fractures and at the upper, or more rarely, lower margin of the massive sulfides). The preponderance of selvedge development at the *upper* margin of the massive-sulfide layer, a feature noted by Woodall & Travis (1969), suggests that pyrrhotite replacement by pyrite was associated with alteration produced by circulating metamorphic fluids in overlying lithologies (see Cowden & Woolrich 1987, Cowden 1986).

DISCUSSION

Fabric elements in massive sulfides

The main fabric elements are summarized below and are illustrated schematically in Figure 8. Development of tectonite fabrics in massive sulfides parallels fabric development in adjacent silicate assemblages (Table 1). As such, the sulfide fabrics reflect the D_1, D_2, D_3 and D_4 deformations, as they formed during both prograde and retrograde metamorphism.

A) The earliest, and least deformed, texture is that of crackle-veined massive sulfide; it contains blobs of fine-grained pyrite in coarse-grained pyrrhotite. This texture may represent a modified primary texture.

B) Pyrrhotite–pentlandite layering, together with flattened, foliated pyrite lenses, represents an S_1 fabric formed in response to strain arising from D_1 thrusting (Fig. 8–2, 3). The pyrite lenses are deformed equivalents of the pyrite aggregates in the crackle-veined massive sulfides.

C) Folding and thrusting associated with the D_2 deformation overprint and transpose S_1 layering, and result in the development, in many instances, of a new S_2 layering. In extreme cases, the only relics of the S_1 foliation are the lenses of fine-

TABLE 1. SUMMARY OF THE TIMING OF THE MAIN FABRIC ELEMENTS IN MASSIVE ORES

	Pyrrhotite-pentlandite-massive ores	Pyrite
D_1	Flattening/simple shear produces banding in massive ores	Flattening of pyrite concentrations to produce fine-grained foliated pyrite lenses
D_2	New banding developed in higher strain domains such as pinchouts	Relict S_1 foliation in pyrite lenses often at an angle to transposed S_2 banding
D_3	Upright S_3 cleavage, plastic flow of massive ore into low stress situations deforms banding	S_3 cleavage in foliated pyrite lenses
D_4	Recrystallization and annealing of existing fabrics to low temperature equivalents	Sulfurization of pyrrhotite to pyrite at the margins of massive ores and along brittle fractures Recrystallization of pre-existing fine grained pyrite to coarse idioblastic pyrite

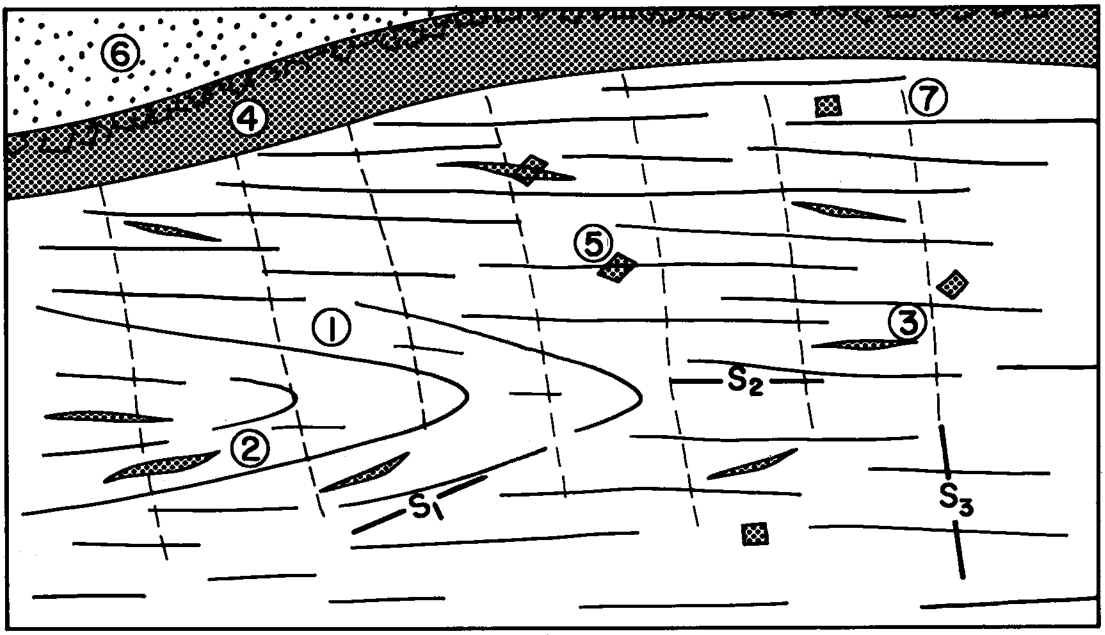

FIG. 8. Schematic representation of major fabric elements and textures of massive sulfides. 1. Pyrrhotite-pentlandite S_1 tectonite banding folded by tight recumbent F_2 fold. 2. Flattened lens of foliated pyrite parallel to S_1 foliation. 3. Transposed pyrrhotite-pentlandite banding defining an S_2 fabric axial planar to F_2 folds. 4. Marginal pyrite band transgressing layering. Note coarse-grained pyrite at upper margin. 5. Idioblastic pyrite overprinting fine-grained pyrite lens and banding. 6. Disseminated sulfides. 7. Upright spaced cleavage (S_3).

grained pyrite inclined at an angle to the transposed S_2 foliation (Fig. 8-2, 3).

D) A weakly developed upright spaced cleavage formed during the D_3 deformation. During or after D_3, fine-grained pyrite replaced pyrrhotite, overprinting existing fabrics along brittle fractures and at the upper margin of the massive-sulfide layer (Fig. 8-4).

E) Brittle fracture of the enclosing rocks modified the overall geometry of the massive-sulfide layer, resulting in plastic flow and contortion of sulfide banding.

F) Idioblastic, coarse-grained pyrite overprints all fabrics and occurs as scattered porphyroblasts in layered sulfides, in the core of pre-existing lenses of fine-grained pyrite and at the upper margin of marginal selvedges of pyrite (Fig. 8-4, 5).

Metamorphic monosulfide solid-solution

Detailed experimental studies in the system Fe-Ni-S (*e.g.*, Naldrett *et al.* 1967, Kullerud *et al.* 1969) contradict our field observations that monomineralic layers were preserved during the peak of metamorphism. Most published experimental data on the system Fe-Ni-S at atmospheric pressure indicate that *Mss* is stable from 300 to 900°C. Consequently, available experimental data on the system Fe-Ni-S have been re-evaluated, incorporating the work of MacDonald and Paterson (pers. comm. 1985) to resolve conflicting experimental data and field observations.

McQueen (1979b) conducted heating experiments on natural Fe-Ni massive-sulfide ores from the Redross mine, a komatiite-associated deposit 50 km south of Kambalda. At 500 and 540°C, his experiments gave conflicting results for different compositions of massive sulfides. Medium-tenor massive sulfides reverted either to Ni-poor *Mss*, or to Ni-poor *Mss* + Ni-rich *Mss*, whereas high-tenor ores reverted to Ni-rich *Mss* + pentlandite assemblages. McQueen's data are summarized in Figure 9, along with our interpreted phase-relationships. It appears that both pentlandite and *Mss* are stable at these temperatures and, most importantly, a complete solid-solution between pyrrhotite and Ni-rich *Mss* does not exist. The conflicting results of the experiments of McQueen (1979a) and Kullerud *et al.* (1969) may reflect kinetic problems in attaining equilibrium in these systems. For example, Barker & Parks (1983) held an Fe-Ni sulfide assemblage at 300°C for two years and found that equilibrium was still not attained and that the field of *Mss* is much narrower than that predicted by Naldrett *et al.* (1967). Thus, incomplete solid-solution between the *Mss* end mem-

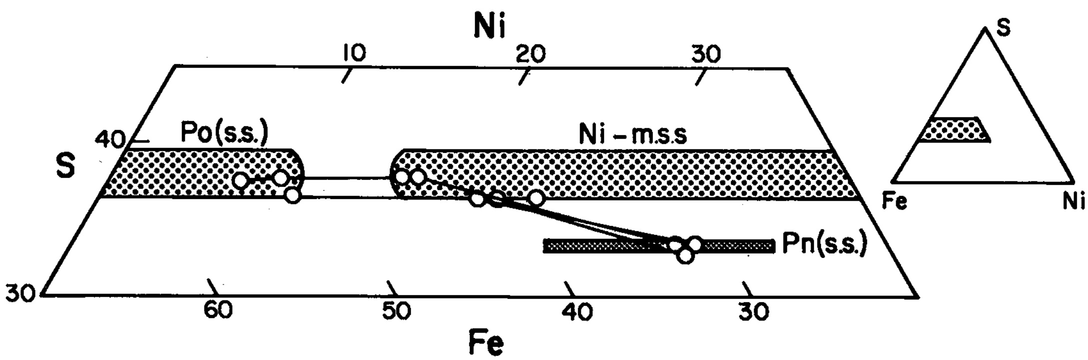

FIG. 9. Portion of the system Fe–Ni–S at 500 to 540°C and one atmosphere, showing our interpreted phase-relationships and the results of McQueen's (1979b) experiments (open circles). Stable assemblages for low- and medium-tenor compositions are Ni-poor *Mss* (Po solid solution + Ni-rich *Mss)*, and Ni-rich *Mss* + pentlandite for high-tenor compositions.

bers may be due to disequilibrium in experiments. Conversely, if equilibrium was achieved, it indicates that two discrete *Mss* phases can coexist at these temperatures. Additional components in the system Fe–Ni–S may also enhance the stability of two *Mss* phases. Hill (1983, 1984) demonstrated that for typical compositions of magmatic sulfide, the presence of only 1% Cu in the system could markedly alter phase relations as the stability of pyrite and pentlandite is enhanced.

Peak metamorphic conditions at Kambalda reached lower-amphibolite facies, and ore textures indicate considerable strain. Of particular relevance, therefore, are the results of an unpublished series of experiments conducted on natural Fe–Ni sulfide ores and their host rocks (J. Macdonald & M. Paterson, pers. comm. 1985). At 600°C with a confining pressure of 3 kbar and a strain rate of 10^{-5} s^{-1}, single-phase *Mss* was not the stable assemblage. The results of these experiments are summarized in Figure 10, which shows that for high-tenor ores, the stable assemblage at 500 to 600°C is Ni-rich *Mss* ± pyrite and for low- and medium-tenor ores, Ni-poor *Mss* + Ni-rich *Mss* ± pyrite. These phase relationships explain the apparent contradiction between our interpretation of the fabric elements and ore textures and the experimental data cited by other investigators. In the case of low- and medium-tenor ores, two *Mss* phases ± pyrite ± pentlandite form the stable assemblage at peak metamorphic conditions. Therefore the ores can deform as bi- or trimineralic aggregates, even at elevated temperatures. The basic requirements for the development of layering are therefore satisfied. Layering developed during prograde metamorphism as Ni-poor *Mss* and Ni-rich *Mss* bands. During retrograde metamorphism, these phases reverted through diffusion-controlled exsolution to the stable low-temperature phases, pyrrhotite and pentlandite. At the same time, prograde fabrics in high-tenor sulfides may be destroyed by reversion to a single Ni-rich *Mss* phase, although pyrite layers and lenses would be preserved. Consequently, many high-tenor ores consist of strongly annealed and recrystallized pentlandite and have only poorly defined tectonite fabrics.

CONCLUSIONS

The major conclusions of this study are listed below, and a summary of the timing of various fabric elements in massive sulfides, relative to deformational events, is given in Table 1.

1) During prograde metamorphism, mineralogical layering in pyrrhotite–pentlandite massive sulfides formed as a response to stress, probably predominantly shear stress, across the massive-sulfide layer. The progressive increase in strain and degree of development of layering toward the footwall in some massive sulfides indicates that these rocks were deformed as polymineralic rocks by ductile non-cataclastic deformation. The textures that developed in massive sulfides are largely a function of the degree of strain and recrystallization; as such, the banded sulfides represent blastomylonites and gneisses.

2) The characteristic, small lenses of foliated pyrite common in the massive sulfides are probably deformed relict magmatic pyrite. They are flattened equivalents of amoeboid aggregates of pyrite in crackle-veined sulfides.

3) Development of a tectonite fabric was widespread during the D_1 deformation, leading to the strong pyrrhotite–pentlandite layering of most low- and medium-tenor ores. During the D_2 deformation, development of a new fabric occurred in zones of higher strain, resulting, in extreme cases, in a new transposed layering. Modification of layering dur-

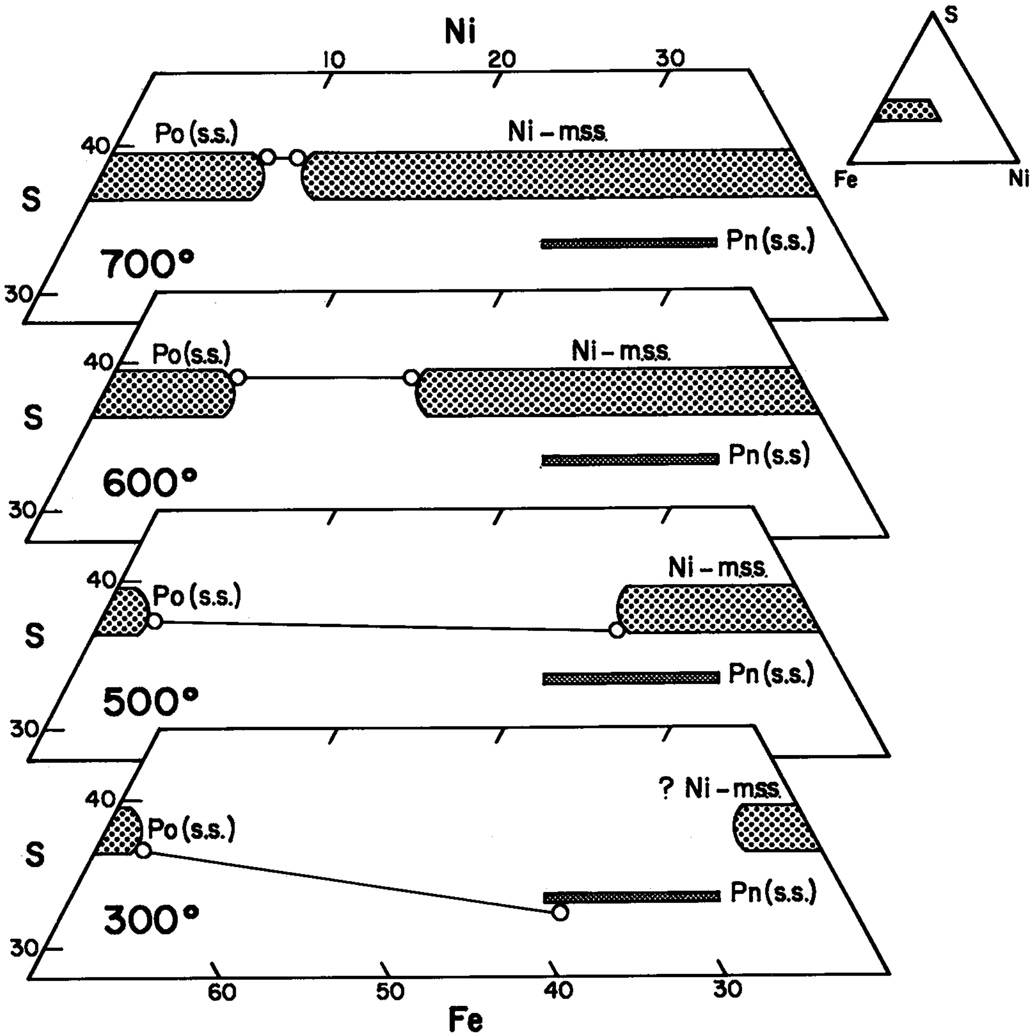

FIG. 10. Portion of the system Fe–Ni–S at 3 kbar confining pressure and a strain rate of 10^{-5} s^{-1}. The diagram illustrates the progressive change in phase relations with temperature. Phase relations are interpreted from mineral compositions (open circles) in products of experiments (data from J. MacDonald and M. Paterson, pers. comm. 1985). Stable assemblages are: 1) 300–500°C: for low-, medium- and high-tenor compositions, Ni-poor *Mss* (Ni-rich pyrrhotite) – pentlandite – Ni-rich *Mss* ± pyrite; 2) 600°C: stable assemblage for low- and medium-tenor compositions is Ni-poor *Mss* – Ni-rich *Mss* ± pyrite, and for high-tenor compositions, Ni-rich *Mss* ± pyrite or pentlandite; 3) 700°C: stable assemblage for low- and medium-tenor compositions is Ni-rich *Mss* ± pentlandite or pyrite.

ing the D_3 deformation resulted in minor development of an upright spaced cleavage without formation of tectonite banding.

4) Sulfur-bearing metamorphic fluids reacted with pyrrhotite at the upper or, more rarely, the lower margin of the massive-sulfide layer to produce a fine-grained pyrite selvedge. Sulfurization occurred simultaneously along zones of brittle fracture transgressing massive sulfides.

5) Coarse idioblastic pyrite developed during metamorphic cooling by recrystallization of fine-grained pyrite of both relict magmatic and replacement types. Other retrograde effects in the massive sulfides were confined to an annealing of fabrics and reversion of high-temperature phases to stable low-temperature phases without significant modification of prograde fabrics.

In summary, the massive Fe–Ni sulfide ores at Kambalda display a range of tectonite fabrics formed through both prograde and retrograde regional metamorphic events; as such, the ores provide a very sensitive record of the tectono-metamorphic history. In low- and medium-tenor ores, bi- or trimineralic assemblages were preserved during the prograde metamorphic events.

ACKNOWLEDGEMENTS

We thank Western Mining Corporation for financial and logistical support, access to the deposits and permission to publish. We are indebted to J. MacDonald and M. Paterson for access to unpublished data on the experimental deformation of nickel sulfides ores and their host rocks. Comments on the manuscript and discussions with D.I. Groves and M. Elias markedly improved the manuscript. Our thanks also to D. Woodman for typing the manuscript and to H. Bush for drafting the figures.

REFERENCES

ARCHIBALD, N.J. (1985): Tectonic and metamorphic history of the Kambalda-Tramways area. *Western Mining Corp., Unpubl. Rep.* **K/2889.**

______, BETTENAY, L.F., BINNS, R.A., GROVES, D.I. & GUNTHORPE, R.J. (1978): The evolution of Archaean greenstone terrains, Eastern Goldfields province, Western Australia. *Precambrian Res.* **6,** 103-131.

BARKER, W. & PARKS, T.C. (1983): The system Fe–Ni–S, thermodynamic and phase equilibria studies. *C.S.I.R.O. Res. Review* **1983,** 58-59.

BARRETT, F.M., BINNS, R.A., GROVES, D.I., MARSTON, R.J. & MCQUEEN, K.G. (1977): Structural history and metamorphic modification of Archaean volcanic-type nickel deposits, Yilgarn Block, Western Australia. *Econ. Geol.* **72,** 1195-1223.

______, GROVES, D.I. & BINNS, R.A. (1976): Importance of metamorphic processes at the Nepean nickel deposit, Western Australia. *Inst. Mining Metall. Trans.* **85** (B), 252-273.

BAVINTON, O.A. (1979): *Interflow Sedimentary Rocks from the Kambalda Ultramafic Sequence: their Geochemistry, Metamorphism and Genesis.* Ph.D. thesis, Australian Nat. Univ., Canberra, Australia.

______ (1981): The nature of sulfidic metasediments at Kambalda and their broad relationships with associated ultramafic rocks and nickel ores. *Econ. Geol.* **76,** 1606-1628.

BAYER, H. & SIEMES, H. (1971): Zur Interpretation von Pyrrhotin-Gefügen. *Mineral. Deposita* **6,** 225-244.

CLARK, B.R. & KELLY, W.C. (1973): Sulfide deformation studies. I. Experimental deformation of pyrrhotite and sphalerite to 2,000 bars and 500°C. *Econ. Geol.* **68,** 332-352.

COWDEN, A. (1986): *The Petrology, Geochemistry and Mineralogy of the Kambalda Iron-nickel Sulfide Deposits, Western Australia.* Ph.D. thesis, Univ. London, London, England.

______ & WOOLRICH, P. (1987): Geochemistry of the Kambalda iron–nickel sulfides: implications for models of sulfide–silicate partitioning. *Can. Mineral.* **25,** 21-36.

DONALDSON, M.J. (1983): *Progressive Alteration of Weakly Mineralised Archaean Dunites from Western Australia.* Ph.D. thesis, Univ. Western Australia, Perth, Australia.

EWERS, W.E. & HUDSON, D.R. (1972): An interpretive study of a nickel–iron sulfide ore intersection, Lunnon shoot, Kambalda, Western Australia. *Econ. Geol.* **67,** 1075-1092.

GRESHAM, J.J. (1986): Depositional environments of volcanic peridotite-associated nickel deposits with special reference to the Kambalda Dome. *In* Geology and Metallogeny of Copper Deposits (G. Friedrich, A. Genkin, A.J. Naldrett, J.D. Ridge, R.H. Sillitoe & F.M. Vokes, eds.). Springer-Verlag, Berlin.

______ & LOFTUS-HILLS, G.D. (1981): The geology of the Kambalda nickel field, Western Australia. *Econ. Geol.* **76,** 1373-1416.

GROVES, D.I., BARRETT, F.M. & MCQUEEN, K.G. (1979): The relative roles of magmatic segregation, volcanic exhalation and regional metamorphism in the generation of volcanic-associated nickel ores of Western Australia. *Can. Mineral.* **17,** 319-336.

______ & HUDSON, D.R. (1981): The nature and origin of Archaean stratabound volcanic-associated nickel–iron–copper sulfide deposits. *In* Handbook of Stratabound and Stratiform Ore Deposits (K.H. Wolf, ed.). Elsevier, Amsterdam.

HILL, R.E.T. (1983): Phase relationships in a portion of the Fe–Ni–Cu–S system which have application to the study of natural nickel–copper ores. *C.S.I.R.O. Res. Review* **1983,** 53-55.

______ (1984): Experimental study of phase relations at 600°C in a portion of the Fe–Ni–Cu–S system and its application to natural sulphide assemblages. *In* Sulphide Deposits in Mafic and Ultramafic Rocks (D.L. Buchanan & M.J. Jones, eds.). Inst. Mining Metall., London.

HUPPERT, H.E., SPARKS, R.S.J., TURNER, J.S. & ARNDT, N.T. (1984): Emplacement and cooling of komatiite lavas. *Nature* **309,** 19-22.

KATZ, M. (1968): The fabric of the granulites of Mont Tremblant Park, Quebec. *Can. J. Earth Sci.* **5,** 801-812.

KULLERUD, G., YUND, R.A. & MOH, G.H. (1969): Phase relations in the Cu-Fe-S and Fe-Ni-S systems. *In* Magmatic Ore Deposits (H.D.B. Wilson, ed.). *Econ. Geol., Mon.* **4**, 323-343.

LESHER, C.M., ARNDT, N.T. & GROVES, D.I. (1984): Genesis of komatiite-associated nickel sulfide deposits at Kambalda, Western Australia: a distal volcanic model. *In* Sulphide Deposits in Mafic and Ultramafic Rocks (D.L. Buchanan & M.J. Jones, eds.). Inst. Mining Metall., London.

______, LEE, R.F., GROVES, D.I., BICKLE, M.J. & DONALDSON, M.J. (1981): Geochemistry of komatiites from Kambalda, Western Australia. I. Chalcophile element depletion – a consequence of sulfide liquid separation from komatiitic magmas. *Econ. Geol.* **76**, 1714-1728.

MARSTON, R.J. (1984): Nickel mineralization in Western Australia. *Geol. Surv. W. Aust., Mineral Resources Bull.* **14.**

______, GROVES, D.I., HUDSON, D.R. & ROSS, J.R. (1981): Nickel sulfide deposits in Western Australia: a review. *Econ. Geol.* **76**, 1330-1363.

______ & KAY, B.D. (1980): The distribution, petrology and genesis of nickel ores at the Juan complex, Kambalda, Western Australia. *Econ. Geol.* **75**, 546-565.

MCQUEEN, K.G. (1979a): *Metamorphism and Deformation of Volcanic-Associated Nickel Deposits: A Study of Mineralization Around the Widgiemooltha Dome, Western Australia.* Ph.D. thesis, Univ. Western Australia, Perth, Australia.

______ (1979b): Experimental heating and diffusion effects in Fe-Ni sulfide ore from Redross, Western Australia. *Econ. Geol.* **74**, 140-148.

MYERS, J.S. (1978): Formation of banded gneisses by deformation of igneous rocks. *Precambrian Res.* **6**, 43-64.

NALDRETT, A.J., CRAIG, J.R. & KULLERUD, G. (1967): The central portion of the Fe-Ni-S system and its bearing on pentlandite exsolution in iron-nickel sulfide ores. *Econ. Geol.* **62**, 826-847.

OSTWALD, J. & LUSK, J. (1978): Sulfide fabrics in some Ni-sulfide ores from Kambalda, Western Australia. *Can. J. Earth Sci.* **15**, 501-515.

PHILLIPS, G.N. & GROVES, D.I. (1984): Fluid access and fluid – wall rock interaction in the genesis of the Archaean gold-quartz vein deposit at Hunt mine, Kambalda, Western Australia. *In* Gold '82: The Geology, Geochemistry and Genesis of Gold deposits (R.P. Foster, ed.). Balkema, Rotterdam.

RAMSAY, J.G. & GRAHAM, R.H. (1970): Strain variation in shear belts. *Can. J. Earth Sci.* **7**, 786-813.

ROSS, J.R. & HOPKINS, G.M.F. (1975): Kambalda nickel sulphide deposits. *In* Economic Geology of Australia and Papua New Guinea. I. Metals (C.L. Knight, ed.). *Austral. Inst. Mining Metall., Mon.* **5**, 100-121.

SECCOMBE, P.K., GROVES, D.I., MARSTON, R.J. & BARRETT, F.M. (1981): Sulfide paragenesis and sulfur mobility in Fe-Ni-Cu sulfide ores at Lunnon and Juan Main shoots, Kambalda: textural and sulfur isotopic evidence. *Econ. Geol.* **76**, 1675-1685.

VERNON, R.H. (1974): Controls of mylonitic compositional layering during non-cataclastic ductile deformation. *Geol. Mag.* **111**, 121-123.

WOODALL, R. & TRAVIS, G.A. (1969): The Kambalda nickel deposits, Western Australia. *Proc. 9th Commonw. Mining Metall. Congr.* **2**, 517-533.

Received October 16, 1985, revised manuscript accepted June 7, 1986.